Sliding Wear and mechanical Properties of Alumina/Glass Fabric/Epoxy Composites

E-glass · sliding wear · specific wear rate · coefficient of friction · Al_2O_3 · mechanical property

In this study, laminates of neat glass fabric/epoxy composite (GEC) and three levels of Al_2O_3 filled glass fabric/epoxy composites, designated as 3AGEC, 6AGEC and 9AGEC (micro particulates of Al_2O_3 - by 3, 6 and 9 wt. % of resin respectively) were prepared using hand lay-up method. 3AGEC exhibits higher tensile strength, flexural strength and flexural modulus besides improved hardness compared to GEC, 6AGEC and 9AGEC. 3AGEC exhibits the lowest specific wear rate compared to GEC, 6AGEC and 9AGEC at all the three loads (i.e., 15, 30 and 45 N) and at a constant sliding velocity of 3.5 $m \cdot s^{-1}$ for a sliding distance of 1.5 km. It was found that beyond filler content of 3 wt. % is deteriorates the mechanical and sliding wear properties of the composites due to agglomeration of the filler. Also, it was found that lowest factor signifies lowest specific wear rate in both neat and all the Al2O3 filled composites.

Gleitverschleiß und mechanische Eigenschaften von Aluminum/Glasgewebe/Epoxy-Komposite

E-Glas · Gleitverschleiß · spezifische Abriebrate · Reibungskoeffizient · Al_2O_3 · Mechanische Eigenschaften

In dieser Arbeit wurden Laminate aus reinen Glasfaser/Epoxy-Kompositen (GEC) und in drei Stufen mit Al_2O_3 - gefüllte Glasfaser/Epoxy-Kompositen, bezeichnet als 3AGEC, 6AGEC und 9AGEC (Mikro Partikel von Al_2O_3 - by 3, 6 und 9 Gew. % jeweils in Harz), in einer manuellen Einlegemethode hergestellt. Die mechanische Charakterisierung und trockene Reibversuche wurden für GEC, 3AGEC, 6AGEC und 9AGEC gemäß ASTM-Normen durchgeführt. Das 3AGEC-Material zeigt im Vergleich zu GEC, 6AGEC und 9AGEC eine höhere Zugfestigkeit, Biegesteifigkeit und Biegemodul neben verbesserter Härte. Die spezifische Abriebrate und die Reibkoeffizienten wurden untersucht.

Figures and Tables:
By a kind approval of the authors.

Introduction

Polymers and their composites form a very important class among tribo-engineering materials. They are used in applications where wear performance in non-lubricated conditions is a key parameter [1]. To make polymer composites suitable for tribological applications researchers have used fillers/whiskers/short or long fibres as reinforcements in polymer matrices (thermoset or thermoplastics) [2-4]. Also, incorporation of micro or nano sized fillers (abrasives or solid lubricants) along with unidirectional and bi-directional woven cloth in a polymer matrix could enhance its mechanical as well as tribological properties [5-8]. Many investigations have been conducted with fibres and fillers of various shapes, sizes, types and compositions in a variety of polymer matrices and it has been proven that wear resistance of polymers improves by the addition of filler(s) and/or fibre(s) [2-8].

Woven fabric reinforced polymer composites have been widely used in many engineering applications in marine, aerospace, automobile, construction and defence sectors as a structural material [9]. Also, in applications, such as circuit boards, switch gear parts, electrical insulating materials in power generation and distribution systems, machine elements like gears, cams, wheels, brakes, clutches, bearings, bushes, leaf springs and levers which were made of conventional metals and particulate polymer composites have been replaced by woven fabric composites. This is because of their ease of use, improved structural performance, reduced cost, better resistance to impact and deformation behaviour, which is closer to that of fully isotropic materials compared to other types of polymer matrix composites [9]. But in many applications, components made of polymer composites come in contact with metals, ceramics and metal composites, and are subjected to relative motion between them, leading to sliding wear and failure of the components. Hence, resistance to sliding wear and low coefficient of friction are the properties emphasized in design of materials for components, which are subjected to sliding action, in addition to other mechanical and functional properties [10]. Abrasives (particulates of SiO_2, Al_2O_3, SiC etc.,) and solid lubricants [particulates of graphite, $MoSO_2$, poly(tetrafluoroethylene) and ultra-high molecular weight polyethylene] were used as wear resistant fillers by many researchers [2, 4, 7- 8, 11-13] in designing polymer composites for tribological applications. Friedrich et al. [10] reported that epoxy filled with the tungsten carbide powder had higher wear resistance than that filled with silica. Ray et al. [14] studied friction and wear behaviour of neat and fly ash filled vinyl ester resin. They concluded that better wear resistance is exhibited by a vinyl ester composite containing 40 wt. % fly ash. Experimental investigations by Wang et al. [15] proved that graphite is more beneficial filler than nano-SiO_2 in improving the tribological properties of basalt fabric composites.

Better chemical and thermal stability, good strength, resistance to wear, electrical insulation and bio compatibility, combined with availability in abundance have made Al_2O_3 an attractive material. It is used in engineering applications like spark plugs, tap washers, pump seals,

Authors:

B. Shivamurthy, S. Anandhan, K. Udaya Bhat, Surathkal, Mangalore, India

Corresponding Author:
K. Udaya Bhat
Department of Metallurgical and Materials Engineering
National Institute of Technology Karnataka
Srinivas Nagar, Surathkal,
Mangalore-575 025, India
Phone: +91-824-2474000
(Ext: 3761)
Fax: +91-824-2474059
E-mail: udayabhatk@gmail.com

KGK RUBBERPOINT

Discover more interesting articles and news on the subject!

www.kgk-rubberpoint.de

Entdecken Sie weitere interessante Artikel und News zum Thema!

electronic substrates, grinding media, abrasion resistant tiles, cutting tools, body armour and refractory bricks [16], and in medical applications, such as dental materials, bone implants and hip-joints [17]. Al_2O_3 has high hardness, electrical insulation property, chemical inertness and it is relatively non-toxic. These properties make it suitable as a filler material for polymers [11].

Afsharimani et al. [12] reported that on addition of Al_2O_3 to poly methyl methacrylate (PMMA) and polystyrene (PS) matrices, their moduli get increased by 107 and 109%, respectively. Also, the surface of Al_2O_3/PMMA composite became more hydrophobic than PMMA alone. Rashid et al. [13] reported an increase in flexural modulus of Al_2O_3/epoxy composite compared to neat epoxy. Ahmed et al. [18] reported that Al_2O_3 filled jute/epoxy composites have better wear resistance than SiC filled jute/epoxy composites. Peng et al. [19] investigated the effects of Al $(OH)_3$ powder on the wear behaviour of glass fibre reinforced epoxy composites. They reported that addition of Al $(OH)_3$ particles up to 6 wt. % decreases the surface temperature, friction coefficient and wear loss of the composites due to absorption of heat by Al $(OH)_3$ particles. The composites with 9 wt. % of Al $(OH)_3$ particles showed increased surface temperature, coefficient of friction and wear loss due to agglomeration.

From literature, it is observed that further scope is there to investigate wear behaviour of Al_2O_3 filled bi-directional woven glass fabric reinforced epoxy composites. In the present work an attempt is made to investigate the effect of Al_2O_3 content in the glass fabric reinforced epoxy composite on specific wear rate, friction coefficient and mechanical properties.

Experimental

Materials

Composites were fabricated from a bi-directional, plain-woven E-glass fabric (with an arial density of 201-203 g.m^{-2} and thickness of 0.17 - 0.19 mm) obtained from Montex Glass Fibre India Pvt. Ltd., India, as the reinforcement. Epoxy resin (LY556), hardener (HT907) and accelerator (DY062) were supplied by Huntsman polymers, Germany. Approximately spherical shaped alumina of particle size range of 8-28 micrometres was used as filler, which was obtained from Jyothi chemicals, India.

1 Material combination and physical properties of neat and Al_2O_3 filled glass/epoxy composites.

Material Code	Constituents (Wt. %)			Density (g.cm^{-3})		Voids (%)
	E-Glass	Epoxy	Al_2O_3	Theoretical	Actual	
GEC	50	50	0	1.636	1.630	0.36
3AGEC	50	47	3	1.675	1.660	0.90
6AGEC	50	44	6	1.709	1.670	2.3
9AGEC	50	41	9	1.742	1.686	3.2

Composite preparation

The matrix was prepared by mixing epoxy resin and hardener at 60 °C at a v/v ratio of 5:4. Al_2O_3 particles were dried in a hot air oven at 130 °C for 4 hours before mixing them with the matrix resin. Accurately weighed Al_2O_3, followed by 2 wt. % of accelerator, was added to the matrix mixture under constant stirring. Epoxy/glass fabric composites containing 3, 6 and 9 wt. % of Al_2O_3 were prepared by this method. The resin mixture was coated on to each layer of E-glass fabric by a brush and a roller. Sixteen such layers were kept between the pressing platens at a stacking sequence of [(0/90)]. 100 µm thick polyester films were used for mold release and to obtain smooth surface on composite slabs. Resin impregnated fabric stock was pressed in a H-type hydraulic press (capacity 40 T) at a pressure of 0.5 MPa for 2 hours at 140 °C. The composite slabs having a size of 300 mm × 300 mm × 3 mm were post cured for 8 hours at 140 °C and their compositions are as given in Table 1.

Physical and mechanical characterizations of composites

The neat glass fabric/epoxy and that filled with Al_2O_3 were tested and characterized as per ASTM standards. Densities (ρ_a) of the composites were measured according to ASTM: D 792-08 [20] (displacement method) using a Metler electronic weighing balance with an accuracy of ± 0.0001 g.cm^{-3}. The theoretical density (ρ_t) was calculated based on the rule of mixtures as per Equation 1. The void content of the composites was estimated from the difference between the theoretical and actual densities using Equation 2.

$$\rho_t = \frac{1}{(W_f|\rho_f) + (W_m|\rho_m) + (W_p|\rho_p)} \quad (1)$$

Where, W_f, W_m and W_p are the weight % fabric, matrix and alumina particle respectively and ρ_f, ρ_m and ρ_t are the densities of fabric, matrix and particles respectively.

$$\text{Void content} = \frac{\rho_t - \rho_a}{\rho_t} \quad (2)$$

Vickers hardness of all the composite specimens was measured by using a Matsuzawa micro-hardness testing machine (model- MMT-X7A, Japan). A square base diamond indenter was forced in to the specimen surface by applying a load of 1 kg. After the removal of the load, the arithmetic mean of two diagonals of the indentation was measured. The Vickers hardness was calculated by the Equation 3.

$$H_V = 0.1889 \frac{F}{L^2} \quad (3)$$

Where, F is the applied load (N), L is the arithmetic mean diagonal of square impression (mm).

Tensile behaviour was investigated as per ASTM: D 638-10 using a universal

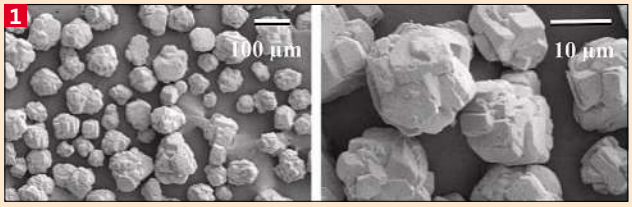

Fig. 1 (a): SEM images of Al_2O_3 particles

Fig. 1 (b) SEM images of E-Glass fabric and individual fibres in the fabric

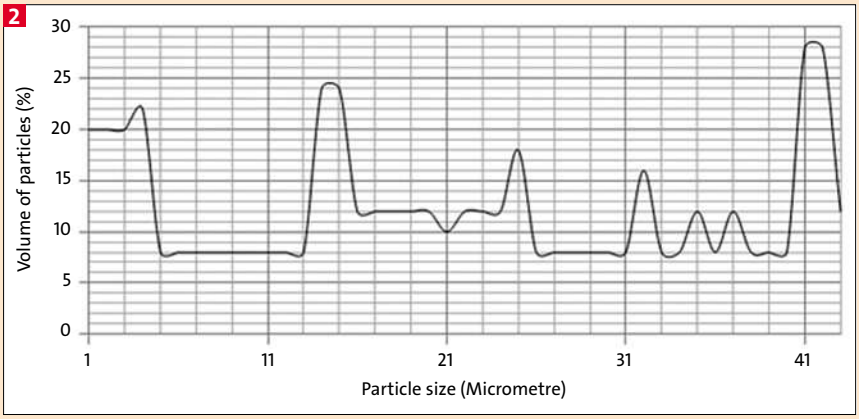

Fig. 2: Particle size distribution of Alumina

testing machine (Instron 3366) [21]. Three point bending technique was adopted to investigate flexural properties of the composites as per ASTM: D 790-10 [22]. The inter-laminar shear strength (ILSS) of these composites was estimated according to classical (Bernoulli-Euler) beam theory using short beam shear (SBS) test as per ASTM: D 2344 [23]. The ILSS was calculated by Equation 4.

$$ILSS = \frac{3F_{max}}{4bd} \quad (4)$$

Where, F_{max} is the maximum load taken by the specimen to fracture (N), b is the specimen width (mm) and d is the specimen thickness (mm). Span to thickness ratio (w/t) equal to 4 was selected for the ILSS test. In each case, to evaluate the physical and mechanical properties, five samples were tested and the average values are reported along with their standard deviations.

Morphology study

A scanning electron microscope (SEM) (model-JEOL-JSM-6380LA, USA) was used to evaluate the texture and morphology of the glass fabric, alumina particles and the composite specimens. The sample surfaces were sputtered with gold in a sputtering unit (model: JEOL JFC 1600, USA), auto fine coater, to make them conductive. The images were taken at suitable accelerating voltages for the best possible resolution, using secondary electron imaging.

Tribological characterization of composites

The sliding wear test was conducted for all the composite samples by using a pin-on-disc machine as per ASTM: G 99-05 [24] with specimens of square shape (size: 10 mm x 10 mm x 3 mm thickness). Sliding speed and sliding distance were fixed as 3.5 $m.s^{-1}$ and 1.5 km, respectively. The normal load was varied as 15, 30 and 45 N. In each case, final weight of the specimen was measured and the wear loss in grams (w) was estimated as the difference of initial weight (w_1) and final weight (w_2). The specific wear rate KS ($g.N^{-1}.m^{-1}$) was calculated by Equation 5.

$$Ks = \frac{w}{F_n \times d} \quad (5)$$

Where, F_n is the normal load (N) and d is the sliding distance (m). The coefficient of friction (μ) was calculated by Equation 6.

$$\mu = \frac{F_f}{F_n} \quad (6)$$

Where, F_f is the frictional force (N).

Results and discussion

Morphology of alumina and glass fabric

Scanning electron microscopic images of Al_2O_3 particles and plain-woven E-glass fabric are shown in Figure 1(a) and 1(b), respectively. Al_2O_3 particles are of approximately spherical shape with irregular surface. The particle size distribution of Al_2O_3 was estimated using IMAGE J software based on SEM pictures and represented as shown in Figure 2. It is observed that the size of particles is approximately is in the range of 8-28 μm. Also, from the SEM investigation of E-glass fabric it is observed that fabric is plain woven type and fibres are free from defects.

Density and voids content of the composites

The theoretical and actual densities of neat and Al_2O_3 filled glass/epoxy composite samples along with the corresponding volume fraction of voids are presented in Table 1. It is observed that the actual density of all the composites is less than the theoretical density. The difference is a measure of voids and pores present in the composites. The void content is less in the control compared to Al_2O_3 filled glass/epoxy composites. This is due to presence of Al_2O_3 in the composite and limitation of the hand layup process [25]. Also, it was observed that the void content in the composites increased with the addition of increased quantity of filler. This is due to the difference of densities of filler and matrix material. However, the void content of all the composites is within the limits.

Hardness

The Vickers hardness values (V_H) of neat and Al_2O_3 filled glass/epoxy composites are shown in Table 2. The hardness value of neat glass/epoxy composite is less than that of the Al_2O_3 filled glass/epoxy composites. Hardness has increased with increased filler content up to 6 wt. %. This is due to reinforcement of the matrix by Al_2O_3 particles. Also, at lower filler loading (3AGEC) better filler dispersion in the matrix contributes to improved bonding between filler, matrix and fibres. This dispersion helps in transferring load acting on the indenter to bottom layers of the laminates effectively (compressive load) and avoids surfaces deformation. At higher filler loading due to the non-homogeneity of the filler dispersion due to agglomeration and presence of voids, lower and variable hardness is observed.

Tensile properties

Tensile behaviour of the neat and Al_2O_3 filled glass/epoxy composites are shown

2 Mechanical properties of neat and Al_2O_3 filled glass/epoxy composites.

Material Code	Tensile properties			Flexural properties		ILSS (MPa)	V_H
	σ_t (MPa)	E_t (GPa)	E (%)	σ_f (MPa)	E_f (GPa)		
GEC	322±3	6.7±0.3	4.8	365±3	16.3±0.5	13.6±0.2	25±2
3AGEC	346±3	6.3±0.3	5.0	425±3	18.8±0.5	14.0±0.2	60±2
6AGEC	285±3	5.6±0.3	5.2	224±3	16.0±0.5	9.8±0.2	62±2
9AGEC	269±3	5.2±0.3	4.5	175±3	15.2±0.5	9.2±0.2	58±2

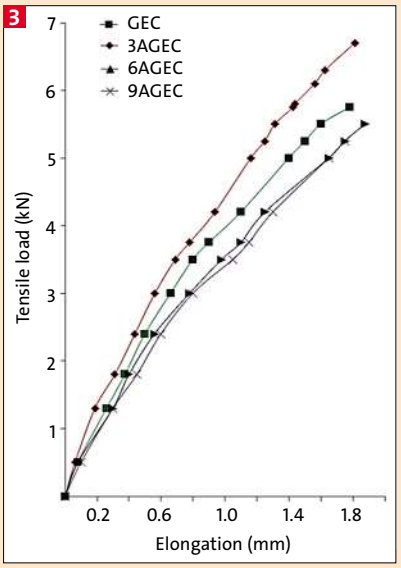

Fig. 3: Tensile load versus elongation curve of neat and Al_2O_3 filled glass/ epoxy composites

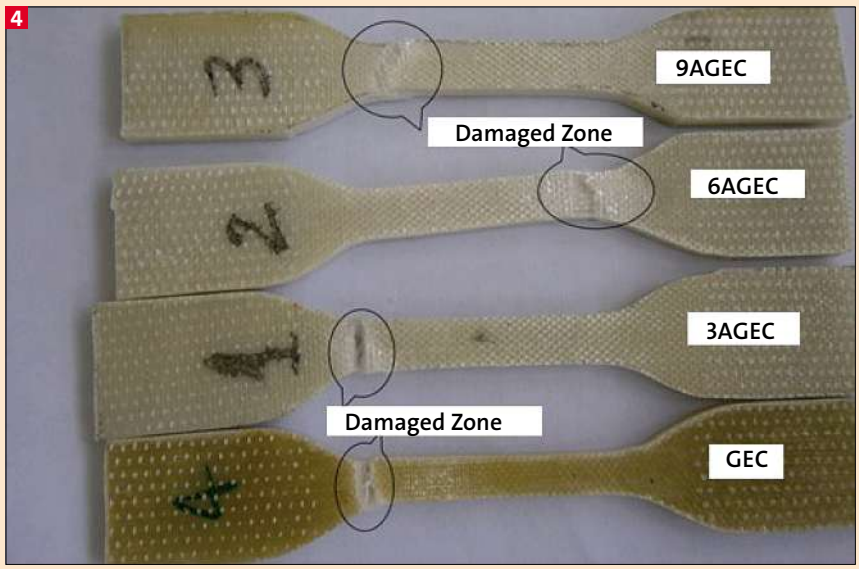

Fig. 4: Digital photographs of fractured tensile specimens of neat and Al_2O_3 filled glass/ epoxy composite

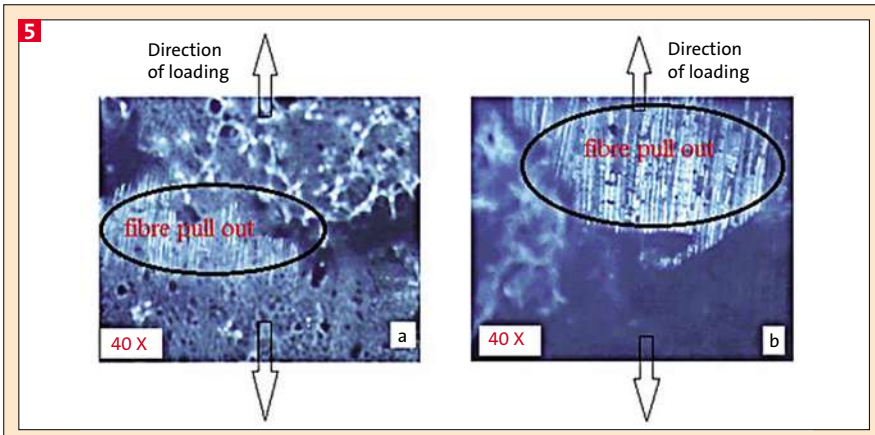

Fig. 5: Microscopic image of fractured tensile specimen of (a) 3AGEC (b) 9AGEC

as load versus elongation plots in Figure 3. The Young's moduli, tensile strength and percentage of elongation are tabulated in Table 2. At 3 wt. % filler loading the changes in elongation and Young's modulus were marginal. But, a slight increase in tensile strength was observed. This is attributed to the irregular surface texture of Al_2O_3 particles (Figure 1(a)), which enhance mechanical interlocking, thereby reducing the slippage of epoxy chains. 6AGEC and 9AGEC exhibit lower tensile strength and moduli compared with GEC and 3AGEC. Higher filler loading in these composites leads to non-uniform dispersion and agglomeration of filler. This develops points of stress concentration in the composites and reduces their strength and moduli. Also, matrix, filler and fibre interaction becomes poorer due to difficulty in wetting of the glass fibre and alumina particles by the epoxy matrix. Hence, load transfer from matrix to reinforcement is not so effective in composites with higher filler content. These two factors cause the composites to fail at lower loads [26].

Figure 4 shows digital photographs of samples, which failed during the tension test. 6AGEC and 9AGEC exhibit a larger damage zone compared to GEC and 3AGEC. Figures 5(a) and 5(b) show fine scale features in the tensile fracture surfaces of 3AGEC and 9AGEC, respectively. Figure 5(a) shows clear indication of fibre breakage without much fibre pull out. Fibre pull out observed in 9AGEC is attributed to poor bonding between the fibre and matrix. Macro view and fracture micrographs indicate that at higher filler loads the load transfer between fibre and matrix is poor and this is attributed to possible agglomeration of fillers and associated improper wetting, stress concentration and voids. These defects lead to early failure during tensile testing.

Flexural strength and flexural modulus

Flexural rigidity is an important property for a laminated composite to resist delamination during service. Flexural modulus and strength were determined by performing three-point bending test and results that are shown in Table 2. But flexural modulus and strength increased on addition of 3 wt. % Al_2O_3. The maximum flexural strength and modulus observed for 3AGEC. This is due mainly to the surface geometry (Figure 1(a)) of the Al_2O_3 particles. The rough surface on these particles creates mechanical interlocking with the matrix that is present between the layers of the glass fabric and gives additional stiffness and flexural strength to the composites. Al_2O_3 particles restrict the mobility of fabric layers over the epoxy matrix and also restrict movement of epoxy chains. Further increase in the filler content beyond 3 wt. % deteriorates the flexural strength due to improper wetting and agglomeration of particles and higher void content.

Inter-laminar shear strength (ILSS)

Inter-laminar shear strength is one of the matrix dominated property in laminated composites [27]. ILSS values of GEC and 3AGEC are almost the same. But, lower ILSS was observed for 6AGEC and 9AGEC. This is also attributed to poor interface between matrix, filler and fibre at higher content of filler.

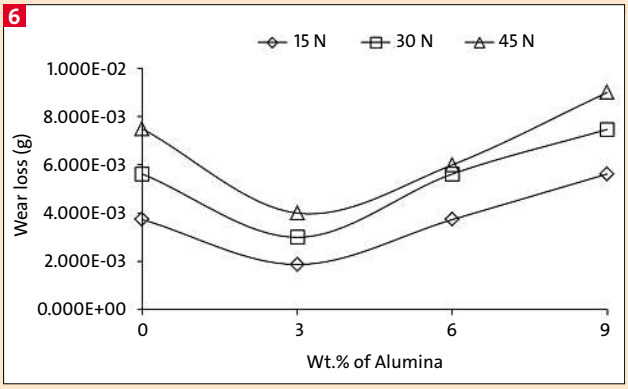

Fig. 6: Wear loss of neat and Al_2O_3 filled glass/epoxy composites at normal loads of 15N, 30N and 45N.

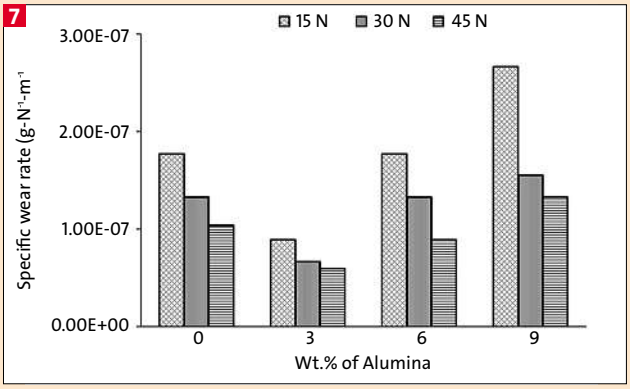

Fig. 7: Specific wear rate of neat and Al_2O_3 filled glass/epoxy composites at normal loads of 15N, 30N and 45N.

Sliding wear behaviour

Wear loss

The effect of applied normal load on the wear loss for all the composites under study is represented by the plots in Figure 6. The control and Al_2O_3 filled glass/epoxy composites exhibited higher wear loss at higher loads. This is due to increased heat build-up in the filler loaded composites due to higher internal friction at higher loads. The high wear loss in the neat glass/epoxy composites is attributed to its low surface hardness. Among Al_2O_3 filled composites 3AGEC exhibits the lowest wear loss at all the three loads. Uniform dispersion of filler in 3AGEC reinforces the hardness and mechanical properties of the matrix as discussed earlier, thereby reducing the wear. At higher filler loading, the structural integrity of the composites is affected by the presence of voids and uneven filler distribution and dispersion. The voids and poor wetting of fibre/fillers helps in dislodging of abrasive particles from the surface and those particles trapped in between the specimen and counter body leads to abrasive wear, in addition to the sliding wear. These are the plausible reasons for the higher wear loss in 6AGEC and 9AGEC.

Specific Wear Rate

Figure 7 shows the specific wear rates of the neat and Al_2O_3 filled glass/epoxy composites at different loads. From this figure, it can be observed that for all the composites the specific wear rate decreases with an increase in the load; this trend is very well pronounced in 6AGEC and 9AGEC than in the control and 3AGEC. This could be attributed to differences in the geometry and texture of glass fibres and Al_2O_3. In general, fibres tend to adhere more strongly to the resin matrix than alumina particles. When specimens are subjected to higher loads, high pressure develops on the wear specimen surface. Due to this, alumina particles are easily dislodged from their positions, whereas, the fibres remain intact, and resist further wear.

3AGEC exhibits the lowest specific wear rate compared to GEC, 6AGEC and 9AGEC at all the three loads. The highest wear rate is observed for 9AGEC. 6AGEC and 9AGEC contain more voids as discussed earlier. Also, the agglomeration of filler reduces its interaction with the matrix and fibres. This creates weaker sections (agglomerated particle zones) and points of stress concentration (voids). When such sections come under sliding, they may not able to withstand surface shear force during the wear testing. Due to this, such specimen surfaces undergo rapid failure in the form of pits and delamination. Further, it adds up to the damage caused by surface defects and thereby increases the wear rate.

3AGEC exhibits the highest tensile and flexural strengths and lower void content compared to other Al_2O_3 filled composites. From the on-going discussions, we can deduce that the specific wear rates of these composites strongly depend on their mechanical properties and the load applied during sliding.

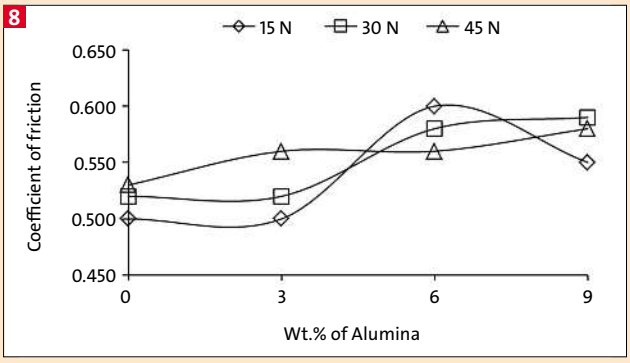

Fig. 8: Coefficient of friction of neat and Al_2O_3 filled glass/epoxy composites at normal loads of 15N, 30N and 45N.

Coefficient of friction

The plots showing the effect of applied load on average coefficient of friction of the neat and Al_2O_3 filled glass/epoxy composites at normal loads of 15, 30 and 45 N are shown in Figure 8. The coefficient of friction increases with an increase in load, and is responsible for the increase in wear loss. It is observed that the coefficient of friction is slightly higher for the Al_2O_3 filled glass/epoxy composites compared to that of control. Also, the coefficient of friction increase with an increases in the content of filler in these composites. This is attributable to the higher hardness of the filler loaded composites compared to the neat matrix. However, 6AGEC and 9AGEC have lower structural property and higher void content. This promotes development of micro cracks on the surface of these composites. Further, when the surface is subjected to sliding action, the agglomerated alumina particles may easily get detached from the surface and get trapped in the wear track. It can promote both adhesive and abrasive wear, which can lead to higher friction between the surfaces. In turn, higher friction promo-

tes localised heat generation, which is not getting dissipated efficiently due to an uneven distribution of Al_2O_3 in these composites. Higher heat build-up disintegrates the polymer surface furthermore and increases the wear. Also, the wear rate in 6AGEC and 9AGEC is decreased with increased normal load. This is, because, at higher loads, the trapped particles in the wear track may get dislodged or crushed, which creates pure adhesive wear. In the case of 6AGEC and 9AGEC, the specific wear rates are higher than that of 3AGEC at all the three loads used. This makes 3AGEC suitable for any applications that require good wear resistance.

Morphology of worn surface

The morphology of the worn surfaces of the hybrid composites is shown in Figures 9-12. Matrix wear was observed in GEC and 3AGEC at a load of 15 N. Debris was formed due to plastic deformation and fracture of matrix and there is no sign of fibre breakage, major cracks and pits (Figures 9(a) and 10(b)). But, in the case of 6AGEC at the same load, small pits were observed, which are due to dislodged portion of agglomerated particles and higher void content (Figure 11(a)). In 9AGEC, multiple fracture of matrix and fibre damage could be observed and this is attributed to severe wear (Figure 12(a)). At a load of 30 N, severe matrix wear was observed along with slight wear of fibre skin in both GEC and 3AGEC (Figures 9(b) and 10(b)). At a load of 30 N, in 6AGEC, more particle detachment from the surface was observed (Figure 11(b)). This is due to higher friction at the spots of particle agglomeration on the resin surface. This, in turn, increases localisation of heat and deformation of matrix around the particles, leading to disintegration of agglomerated particles from the surface. This is visible as patches in the SEM micrographs. This was observed in composites subjected to higher load (Figure 11(c)). Severe fracture of matrix and fibres as well as pit formation was observed in 9AGEC specimens subjected 30 and 45 N loads (Figure 12(b)). In the case of samples subjected to a load of 45 N, additional micro cracking was observed (Figure 12(c)). This is attributed to the higher void content in this composite.

Correlation of mechanical properties with wear

From literature, it is found that the specific wear rates of few polymer composites

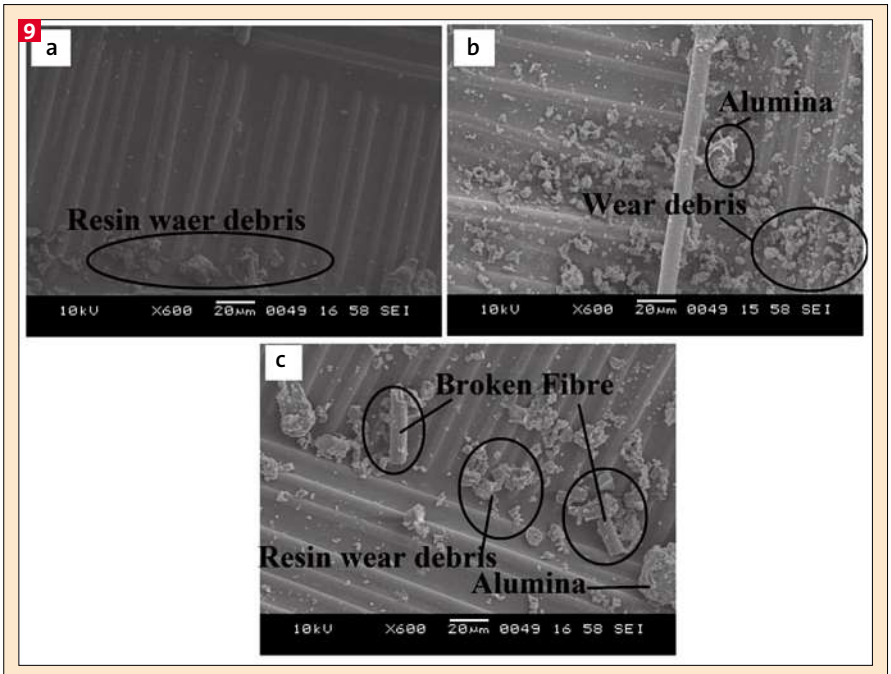

Fig. 9: SEM images of neat glass/epoxy composites at normal loads, (a) 15N, (b) 30N and (c) 45N.

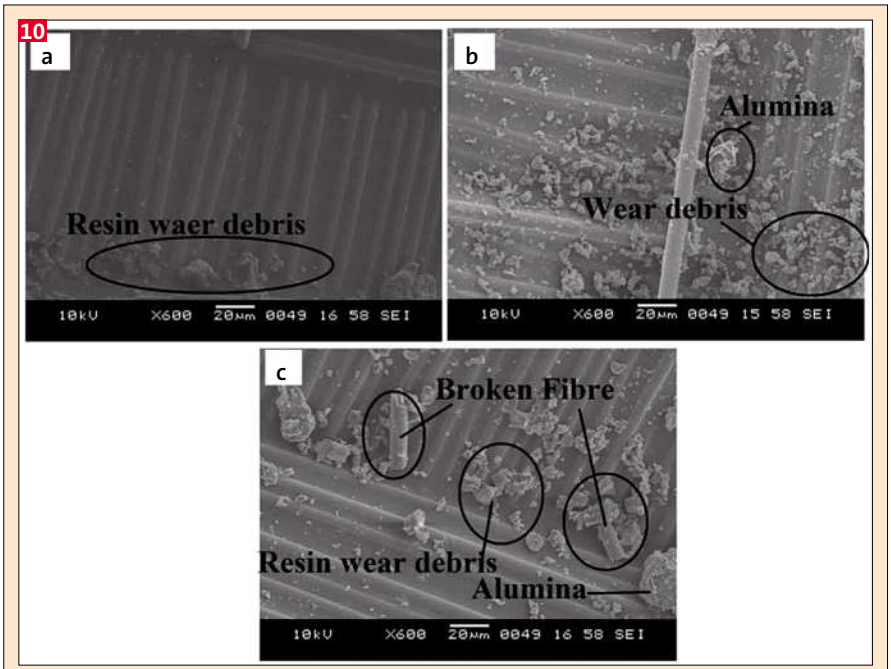

Fig. 10: SEM images of 3AGEC at normal applied loads (a) 15N, (b) 30N and (c) 45N.

are correlated with a factor called Ratner- Lancaster factor [28-30]. It is an inverse of product of tensile strength (σ) and percentage elongation (e) of the polymer composite. The investigation reported by Bijwe et al. [28] on polyethersulfone/aramid composites proved that the specific wear rate in linear relation with Ratner- Lancaster factor $(\sigma.e)^{-1}$. From literature, it was observed that tensile behaviour of a composite exerts a pronounced influence on its wear rate. As the tensile strength and elongation increases, the fracture toughness of a material increases, and more energy is required to deform that material; hence, its wear rate decreases. A similar observation was made in the present study also. 3AGEC exhibits lowest valve of $(\sigma.e)^{-1}$ and lowest specific ware rates (at all the three applied loads) compared to GEC, 6AGEC and 9AGEC.

11

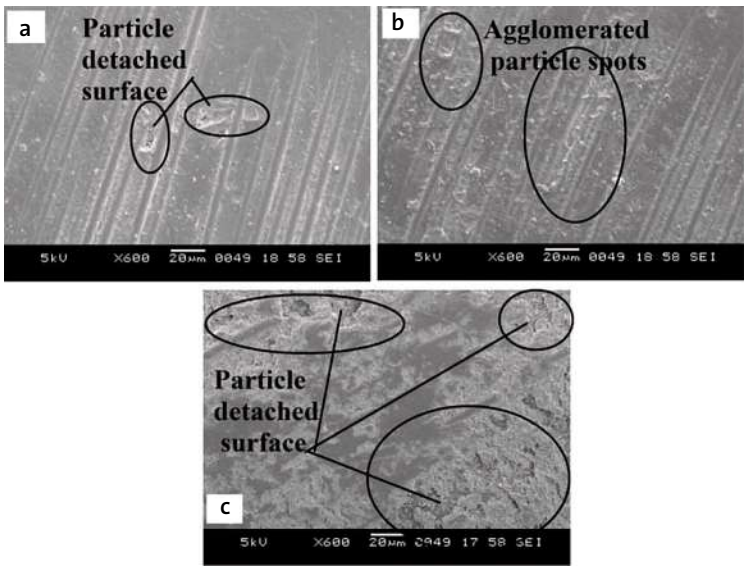

Fig. 11: SEM images of 6AGEC at normal loads (a) 15N, (b) 30N and (c) 45N.

12

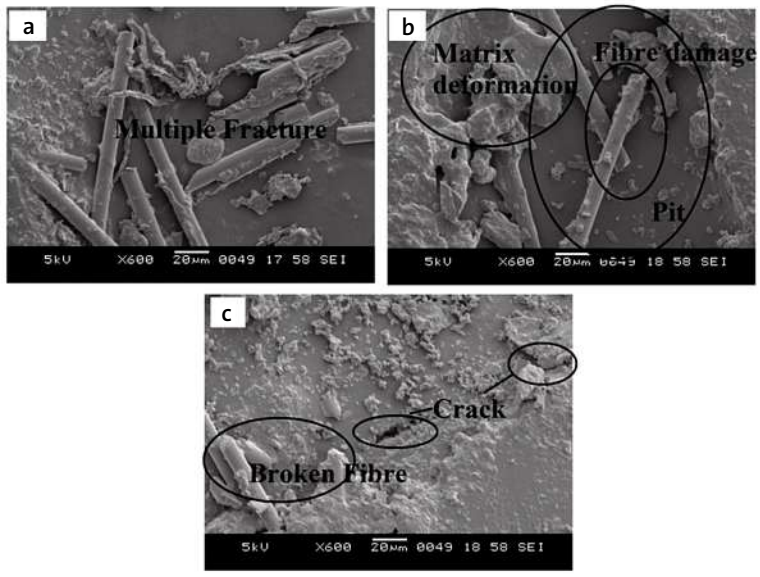

Fig. 12: SEM images of 9AGEC at normal loads (a) 15N, (b) 30N and (c) 45N.

13

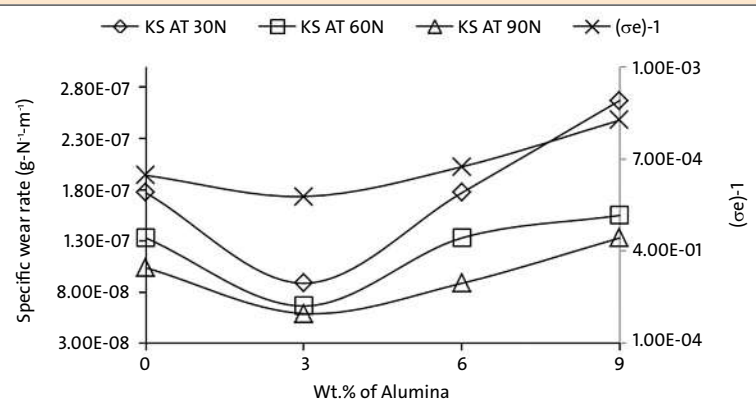

Fig. 13: Plot of specific wear rate and Ratner factor versus Al_2O_3 content in glass/epoxy composites.

Conclusions

From this study, it can be concluded that addition of Al_2O_3 particles to glass fabric/ epoxy composites improves their mechanical properties and wear resistance. Lowest specific wear rate and better mechanical property was observed for the hybrid composites containing 3 wt. % of Al_2O_3. The highest specific wear rate was observed for the hybrid composite containing 9 wt. % of Al_2O_3. In composites loaded with a higher amount of Al_2O_3, non uniform dispersion of filler, voids and agglomeration of the filler particles deteriorate the wear resistance and mechanical properties. It is found that the specific wear rates of the neat and Al_2O_3 filed composites strongly depend on the $(\sigma.e)^{-1}$ factor. The parameters, σ and e, control the wear behaviour of the neat and Al_2O_3 filled glass/epoxy composites.

References

[1] IM. Hutchings, Tribology: Friction and wear of engineering materials. CRC Press, London, 1992.

[2] N. Chand, UK Divedi, MK. Sharma (2007) Development and tribological behavior of UHMWPE filled epoxy gradient composites. Wear **262**:184.

[3] O. Bülent, A. Fazlı, Ö. Sultan (2007). Hot wear properties of ceramic and basalt fiber rein forced hybrid friction materials. Tribol Intern **40**, 37.

[4] G. Xian, R. Walter, F. Haupert (2006) Friction and wear of epoxy-based nano composites: Influence of additional short carbon fibers, aramid and PTFE particles. Compos Sci & Technol **66**: 3199.

[5] B. Suresha, G. Chandramohan, JN. Prakash, K. Balusamy, K. Sankaranarayanasamy (2006). The role of fillers on friction and slide wear characteristics in glass-epoxy composite systems. J. Miner Mater Char Eng **5**: 87.

[6] P. Kishore, S. Sampathkumar, P. Seetharamu, M. Thomas, Janardhana (2005). A study on the effect of the type and content of filler in epoxy-glass composite system on the friction and slide wear characteristics. Wear **259**, 634.

[7] B. Suresha, G. Chandramohan, P. Sampathkumaran, S. Sethuramu (2007). Investigation of the friction and wear behaviour of glass-epoxy composite with and without graphite filler J Reinf.Plast Compos **26**, 81.

[8] B. Shivamurthy Siddaramaiah, M.S. Prabhuswamy (2009) Influence of SiO_2 fillers on sliding wear resistance and mechanical properties of compression molded glass epoxy composites. J Miner Mater Char & Eng 8: 513-530

[9] ASM Handbook, Vol.8, ASM International 1992, Materials Park, Ohio, USA.
[10] Friedrich K. Zhong Z, Schlarb AK (2005) Effect of various fillers on the sliding wear of polymer composites. Compos Sci & Technol **65**, 2329.
[11] Laigui Yu. Bahadur S. Qunji Xue (1998) An investigation of the friction and wear behaviors of ceramic particle filled polyphenylene sulfide composites . Wear **214**, 54.
[12] Afsharimani SN. Zad AI. Tafresh MJ, Salartayefeh S (2010) Synthesis and characterization of alumina flakes/polymer composites. J Appl Poly **115**, 3716.
[13] Rashid ESA., Ariffin K. Kooi CC, Akil (2008) Mechanical and thermal properties of polymer composites for electronic packaging application. J Polym Res **27**, 1573.
[14] Ray D, Gnanamoorthy R (2007) Friction and wear behaviour of vinyl ester resin matrix composites filled with flyash particles. J Reinf Plast Compos. **26**, 5.
[15] Wang Q H. Zhang XR,Pei XQ (2010) Study on the friction and wear behavior of basalt fabric composites filled with graphite and nano-SiO_2. Materials & Design **31**, 1403.
[16] Morrell R. Hand book of properties of technical and engineering ceramics part-2, 1987. Data reviews, Section I, High- Alumina Ceramics, London.
[17] Thamaraiselvi TV, Rajeswari S (2004) Biological evaluation of bio ceramic materials - A review. Trends Bio mater Artif Organs **18**, 9.
[18] Ahmed KS. Khalid SS. Mallinatha V, Amith Kumar SJ (2011) Dry sliding wears behavior of SiC/Al_2O_3 filled jute/epoxy composites. Materials & Design **36**, 306.
[19] Guirong P. Gao L. Zhan Z. Wang H, Hao W (2009) Wear behaviour of Al(OH)3-GF/epoxy composites in low velocity. Polym Bull **63**, 911.
[20] ASTM D 792- 08, Standard test methods for density and specific gravity (relative density) of plastics by displacement, ASTM International, June 2012.
[21] ASTM D 638-10, Standard test method for tensile properties of plastics, ASTM International, June 2012.
[22] ASTM D7 90-10, Standard test methods for flexural properties of unreinforced and reinforced plastics and electrical insulating materials, ASTM International, June 2012.
[23] Adams DF, Lewis EQ (1997) Experimental assessment of four composite material shear test methods. J Test Eval **25**, 174.
[24] ASTM G 99 – 05, Standard test method for wear testing with a pin-on-disk apparatus, August 2012.
[25] Patnaik A, Satapathy A, Biswas S (2010) Investigations on three-body abrasive wear and mechanical properties of particulate filled glass epoxy composites. Malay Poly J **5**: 37.
[26] Hussain M, Nakahira A, Niihara K (1996) Mechanical property improvement of carbon fiber reinforced epoxy composites by Al_2O_3 filler dispersion. Mater Lett **26**: 185.
[27] Feraboli P, Kedward KT (2003) Four-point bend interlaminar shear testing of uni- and multi-directional carbon/epoxy composite systems. Composites: Part A **34**: 1265.
[28] Bijwe J. Awtade S. Satapathy. BK. Ghosh AK (2004) Influence of concentration of aramid fabric on abrasive wear performance of polyethersulfone composites. Tribo Lett **17**, 187.
[29] Mohan N. Natarajan S. Kumaresh. Babu SP, Siddaramaiah (2010) Investigation on sliding wear behaviour and mechanical properties of jatropha oil cake-filled glass-epoxy composites. J Am Oil Chem Soci **88**,111.
[30] Poomalai P. Siddaramaiah, Suresha B, Lee JH (2008) Mechanical and three-body abrasive wear behaviour of PMMA/TPU blends. Mater Sci & Eng - A **492**, 486.